INSTITUT DE FRANCE
Académie des sciences

Comptes Rendus
Physique

Sha Han, Can-Li Song, Xu-Cun Ma and Qi-Kun Xue

Interface enhanced superconductivity in FeSe/$SrTiO_3$ and the hidden nature

Volume 22, Special Issue S4 (2021), p. 163-182

Published online: 5 October 2021
Issue date: 8 March 2022

https://doi.org/10.5802/crphys.87

Part of Special Issue: Recent advances in 2D material physics
Guest editors: Xavier Marie (INSA Toulouse, Université Toulouse III Paul Sabatier, CNRS, France) and Johann Coraux (Institut Néel, Université Grenoble Alpes, CNRS, France)

Les Comptes Rendus. Physique *sont membres du*
Centre Mersenne pour l'édition scientifique ouverte
www.centre-mersenne.org
e-ISSN : 1878-1535

Comptes Rendus
Physique
2021, 22, nº S4, p. 163-182
https://doi.org/10.5802/crphys.87

Recent advances in 2D material physics / *Physique des matériaux bidimensionnels*

Interface enhanced superconductivity in FeSe/SrTiO$_3$ and the hidden nature

Sha Han[a, b], **Can-Li Song**[a, c], **Xu-Cun Ma**[*, a, c] **and Qi-Kun Xue**[*, a, c, d, e]

[a] State Key Laboratory of Low-Dimensional Quantum Physics, Department of Physics, Tsinghua University, Beijing 100084, China

[b] CAS Key Laboratory of Nanophotonic Materials and Devices, Suzhou Institute of Nano-Tech and Nano-Bionics, Suzhou 215123, China

[c] Frontier Science Center for Quantum Information, Beijing 100084, China

[d] Beijing Academy of Quantum Information Sciences, Beijing 100193, China

[e] Southern University of Science and Technology, Shenzhen 518055, China

E-mails: shan2020@sinano.ac.cn (S. Han), clsong07@mail.tsinghua.edu.cn (C. L. Song), xucunma@mail.tsinghua.edu.cn (X. C. Ma), qkxue@mail.tsinghua.edu.cn (Q. K. Xue)

Abstract. The superconductivity confined in a two-dimensional interface exhibits many exotic phenomena that have certain counterparts in layered cuprates and iron-based superconductors, and thus provides rare opportunities to reveal the mystery of high temperature superconductivity therein. By constructing and tailoring hybrid heterostructures such as FeSe/SrTiO$_3$ (FeSe/STO), interface-enhanced superconductivity arouses, and the substrate has been demonstrated to provide the phonons and enhance the strong electron–phonon coupling (EPC) within monolayer FeSe. More research and reporting systems uncover that the band-bending induced charge transfer at the interface could become a unified microscopic picture to design the new interface superconductors. With re-examination of the experimental research in LaAlO$_3$/STO (LAO/STO) and unconventional superconductors, the common characteristics such as band bending and rigid band shift are perceived in the FeSe/STO, LAO/STO and cuprate superconductors. This review may provide important information to inspect the mechanism of high-T_c superconductivity from a different view.

Keywords. Interface superconductivity, FeSe/SrTiO$_3$, Band bending, Rigid shift, Electron–phonon coupling, High-T_c superconductivity.

Available online 5th October 2021

* Corresponding authors.

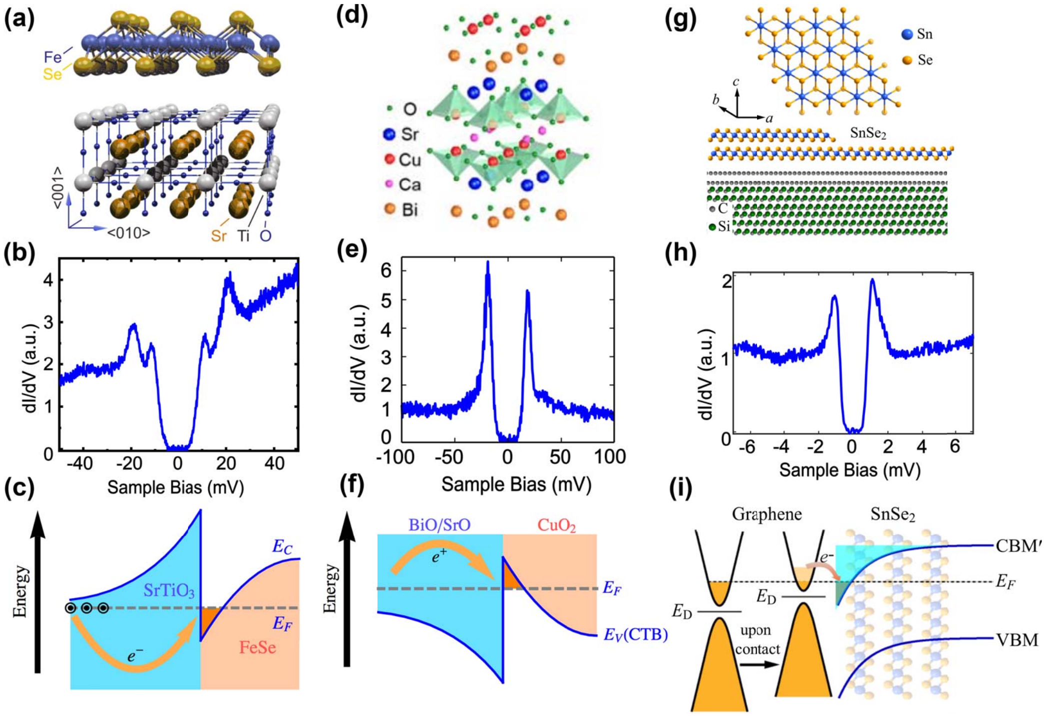

Figure 1. Interface superconductivity in different heterostructures: (a–c) FeSe/STO, (d–f) CuO_2/Bi2212 and (g–i) $SnSe_2$/graphene. Upper panels refer to schematical structure. Middle panels refer to scanning tunneling spectroscopy (STS). Lower panels show the band bending model [1, 24–26].

1. Introduction

Interface-enhanced superconductivity in one-unit-cell FeSe film on STO (1UC FeSe/STO) was discovered in 2012 (Figure 1(a–c)) [1], and subsequently reported with an unexpected high transition temperature (T_c) from 65 K to even 109 K [2–8]. More interestingly, 1UC FeSe/STO possesses a simple Fermi surface topography consisting of only electron pockets at the corner of the Brillouin zone and there are no hole pockets at the zone center [2, 3, 5]. The electron doping and EPC at the FeSe/STO interface are regarded to play roles in the observed high temperature superconductivity [9–15] while others support the spin fluctuations [16–18] for EPC appears to be too weak for the high T_c value [19, 20]. Experiments from neutron scattering [21], Raman [22], isotope effect [23] and so on show that EPC works too. These findings have attracted much attention to concerning superconductivity at interfaces (Figure 1). Compared to the cuprate bulk crystals with a T_c above liquid nitrogen temperature (77 K) in the ambient conditions [12], 1UC FeSe/STO stands for a new interfacial superconductor with the high superconducting temperature above 77 K [13]. This boosts a new frontier for superconductivity and also injects new thoughts on the design of new superconductors experimentally and theoretically in the past years.

Research on 1UC FeSe/STO also has inspired a re-examination of the unconventional superconductors such as cuprates. The cuprate compounds all share the same CuO_2 layer in common, which holds the insulating parent state. The other constituents are generally sorted as the charge reservoirs supplying carriers into the superconducting CuO_2 layers. In such sense the high-T_c complex is nothing more than an infinite repetition of the superconducting/non-superconducting interfaces, belonging to the broad interface superconductivity category as well. Indeed, interface superconductivity was observed in the $La_{2-x}Sr_xCuO_4$ (LSCO)-based bilayer heterostructures [14, 15]. For cuprates with different CuO_2 numbers in unit cell, the stacking situation differs and thus the band alignment varies, leading to the increase of doping efficiency from $n = 1$ to $n = 2$ as shown in Figure 5 in Ref. [27] which shows that maximum T_c is achieved at a lower doping level for $n = 2$. Provided with efficient charge transfer, superconductivity should emerge even for a single isolated interface regardless of modifications outside. In this context, lots of efforts have been devoted to the interface issue between the CuO_2 and charge reservoir layers, including the successful growth of a CuO_2 monolayer on $Bi_2Sr_2CaCu_2O_{8+\delta}$ (Bi2212) and observation of nodeless superconductivity (Figure 1(d–f)) [25]. Note that tri-crystal experiment [28] shows a d-wave gap which is often considered as the evidence for non-conventional mechanism while d-wave gap doesn't necessarily exclude a BCS mechanism [29]. More importantly, the recent experimental result based on high quality of the Josephson junctions of Bi2212 ultrathin flakes strongly favors the scenario of a persistent s-wave order parameter [30]. The modulation-doping induced two-dimensional hole liquid (2DHL) confined in the CuO_2 planes has come into being. In addition, the interface superconductivity in a structurally simple van der Waals heterostructure composed of semiconducting metal dichalcogenide $SnSe_2$ and graphene was realized very recently (Figure 1(g–i)) [26]. A two-dimensional electron gas (2DEG) marked with non-zero density of states (DOS) in the large semiconducting gap was found at the $SnSe_2$/graphene interface, which bears the responsibility for superconductivity observed regardless of the semiconducting nature in bulk $SnSe_2$.

These observations all support that the interfaces benefit from the two materials building them up in a heterostructure, helping the realization of superconductivity in different materials, namely, bad metal (FeSe), Mott insulator (CuO_2), and semiconductor ($SnSe_2$). In order to clarify the mechanism of interface superconductivity in the different systems, several scenarios invoking interfacial strain effect, charge transfer and EPC, are often proposed. However, a unified microscopic picture on how the interface superconductivity is prompted remains puzzling. For this purpose, we not only review the experimental research including spectroscopic study of 1UC FeSe/STO, CuO_2/Bi2212, but also reexamine the previous results of LAO/STO [31] and even cuprate superconductors, and aim to capture the common characteristics among them. The effects of charge transfer and band alignment are discussed first in the four systems. Then the rigid band shift and EPC are examined in the 1UC FeSe/STO, cuprates and LAO/STO systems. The polar nature's influence on LAO/STO and cuprate on the tilted band structure is highlighted. All discussions include the similar token in cuprates and may provide more insights into understanding the mechanism of high-T_c superconductivity in cuprates.

2. Band alignment and doping

2.1. *Band bending in 1UC FeSe/STO*

At present, a series of FeSe-based high-temperature superconductors were found by using gating technique [32], intercalation [33, 34] and surface potassium doping [35–37], which all exhibit the same Fermi surface as that of 1UC FeSe/STO. However, 1UC FeSe/STO is very unique due to the electron doping originated from the band alignment at the interface. The importance of the charge transfer in FeSe/STO is also supported by the absence of superconductivity in FeSe separated by large neutral spacer molecules [38].

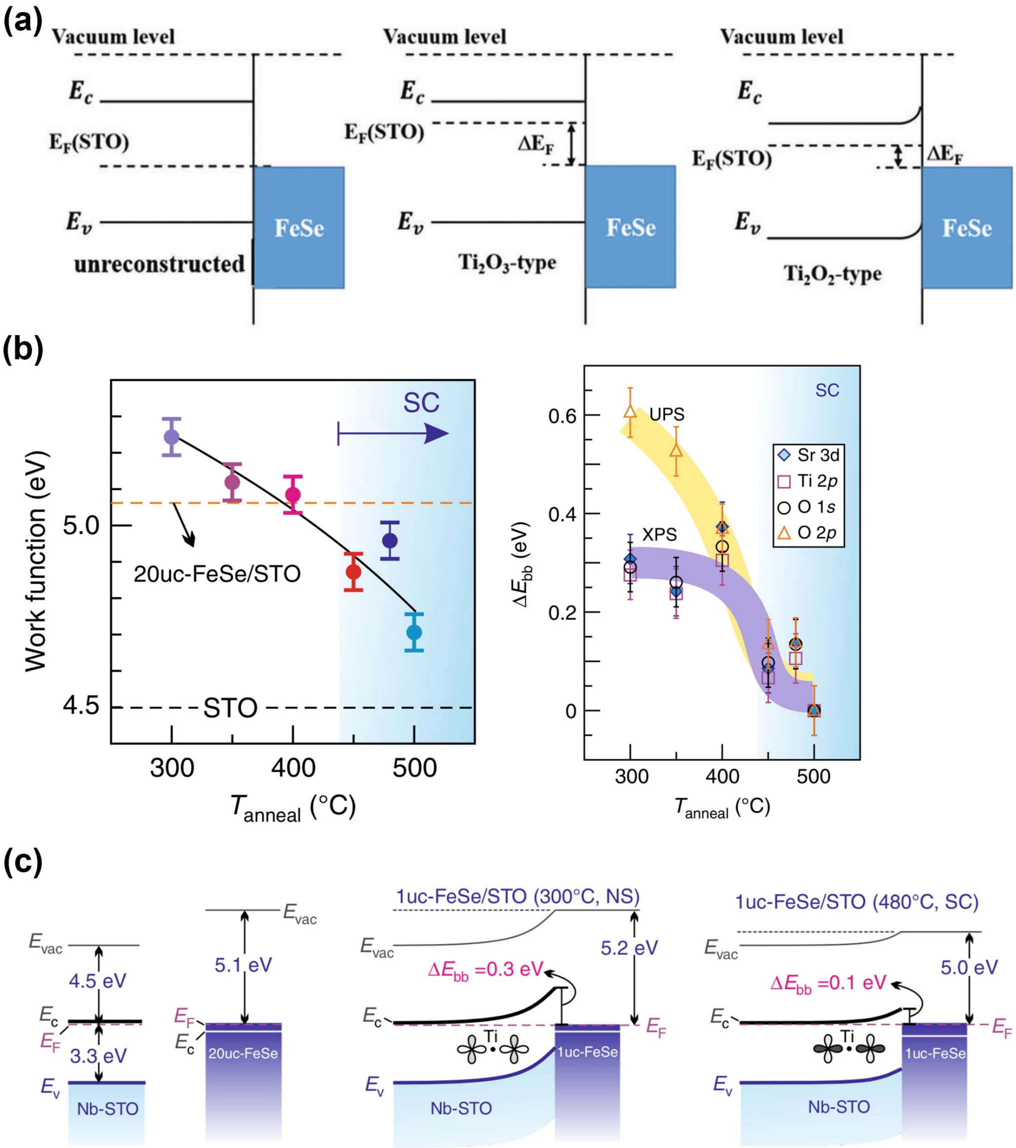

Figure 2. (a) Schematic of band bending of monolayer FeSe deposited on the unreconstructed, Ti_2O_3-type, and Ti_2O_2-type STO reconstructed surfaces [39]. (b) Work function of 1UC FeSe/STO and fitted band bending values as a function of annealing temperature [40]. (c) Energy bands of Nb-doped STO and 20UC-FeSe separately (left), energy band profile across the FeSe/STO heterostructure at the non-superconduting (middle) and superconducting stages (right), respectively. The inset shows cartoons of O 2*p* orbitals. Dark color highlights the bonding strength [40].

The band alignment as the origin of charge transfer in FeSe/STO has long been proposed since the discovery of the interface superconductivity in this system [1], and has been observed by different experimental techniques [40, 41]. Besides, the two-dimensional electron liquid (2DEL) from charge transfer due to band bending detected by the low-energy muon spin rotation/relaxation (μSR) technique is about 6×10^{14} cm^{-2} [42], which is about 1 electron per unit cell. This superfluid density is much larger than the value that the O vacancies or Ti excess [43] can offer. In principles of semiconductor band bending, the Schottky barrier ϕ_{SB} between the metallic FeSe and semiconducting STO is defined as $\phi_{SB} = \phi_{FeSe} - \chi_{STO}$, where ϕ_{FeSe} is the work function of FeSe and χ_{STO} is the electron affinity energy of STO. For STO, χ_{STO} is proportional to the chemical potential. Thus the band bending can be tuned via changing either ϕ_{FeSe} or ϕ_{STO}. Xu *et al.* reported that Ti_2O_3 on the STO is more electron doped compared to Ti_2O_2 on the STO, thus $\phi_{Ti_2O_3} < \phi_{Ti_2O_2}$ (Figure 2(a)) [39]. So the band bends upwards more in Ti_2O_3-type STO. On the other hand, the ϕ_{FeSe} can be tuned by annealing (Figure 2(b)) by which ϕ_{FeSe} decreases [40]. Thus, the Schottky barrier (denoted as ΔE_{bb} in Figure 2(b)) decreases with the increased annealing temperature [40]. The band bending sketch is depicted in Figures 2(c) and 1(c). Similar phenomenon is observed by EELS [41]. Further, the 2DEL from charge transfer due to band bending is confirmed by 4 times value of superfluid density detected by the μSR technique compared with that expected from angle-resolved photoemission spectroscopy (ARPES) measurements [42]. Following the band bending idea, the charge transfer between FeSe and MgO(001) substrate is also investigated [44].

For semiconductors, the carrier density follows the barrier height. Take $Al_xGa_{1-x}As$/GaAs heterostructure for example, the Al doping induces electrons, eliminating the work function of $Al_xGa_{1-x}As$ [40, 45]. Thus the work function difference $\Delta\phi = \phi_{GaAs} - \phi_{Al_xGa_{1-x}As}$ will increase, resulting in the increase of 2DEL in the potential well. However, the carrier density in FeSe/STO, different from the one in $Al_xGa_{1-x}As$/GaAs, increases with the decreasing Schottky barriers. This increase is explained in that annealing changes the stoichiometry of FeSe, which gains a higher electron density with the desorption of extra Se. The abundant Se atoms at the interface are also supported by the larger values from ultraviolet photoemission spectroscopy (UPS) than the ones from element-sensitive X-ray photoemission spectroscopy results at annealing temperatures lower than 400 °C as shown in Figure 2(b) [40]. In a word, both annealing and electron-doping weaken the ϕ_{FeSe} while the carrier density trends oppositely due to the involvement of stoichiometry of FeSe.

Electron doping due to band bending and charge transfer could provide enough charge carriers, one of the key factors for superconductivity of 1UC FeSe/STO. However, excess electrons with strong correlation can't induce the maximum T_c. To realize higher T_c, the efficacy of EPC should also be considered, as discussed in the electron–phonon section.

2.2. *Band bending in cuprates*

The band bending has been utilized to understand the superconductivity between insulating Sm_2CuO_4 (SCO) and semiconducting STO heterostructure [46]. Actually, within cuprates, the band bending between CuO_2 and charge reservoirs is firstly postulated in the CuO_2/Bi2212 system [25] as shown in Figures 1(f) and 3(a). Such charge-transfer mechanism has long been employed as modulation-doping in semiconductor high-electron-mobility-transistors such as $Al_xGa_{1-x}As$/GaAs superlattices [45], as schematically illustrated in Figure 3(b). It is well-established that charge transfer is initiated only when the E_F of doped n-type $Al_xGa_{1-x}As$ is higher than that of undoped GaAs. According to this model, the undoped CuO_2 is a Mott insulator. At critical doping, the superconductivity is induced by the charge transfer from adjacent reservoir layers to CuO_2 because of the E_F difference between CuO_2 and adjacent layers (panel i of Figure 3(a)). This differs from the well-known concept that doping is induced by a change in charge reservoir stoichiometry that pulls out an electron from the CuO_2 plane. A direct deduction of this latter understanding is that the carrier density is equal to the doping level. However, in YBCO the carrier density is about $1 + p$ when doping exceeds 0.19 [47]. This non-linear relation

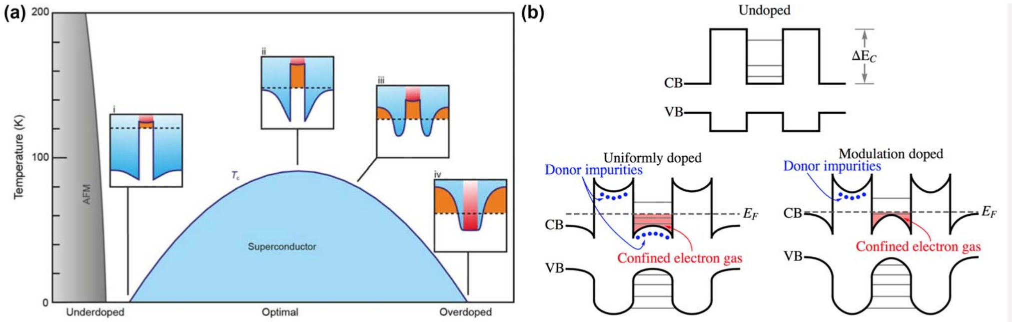

Figure 3. (a) Phase diagram of high-T_c cuprate based on modulation-doping charge transfer in CuO_2/Bi2212 system. Doping changes reservoirs' E_F while CuO_2 remains intact. (b) Energy-band diagrams for undoped (top), uniformly doped (bottom left) and modulation doped (bottom right) GaAs-Al_xGa_{1-x}As superlattices [45].

in cuprates is explained later in part 3 that the carrier density is the arcsine function of the doping level. As for the slope returning to 1 at higher doping levels, it may be connected with the fact that the quantum well has collapsed. Another evidence of the magnification of doping for carrier density has been listed in part 2.1 that the superfluid density detected by the μSR technique is 4 times of the value expected from ARPES measurements [42]. As claimed in Ref. [27], the ARPES gives the value of doping level. Thus, a clean 2DHL is formed in the quantum well between CuO_2 and the reservoirs. Formation of 2DHL doesn't change the electronic ground states of CuO_2 in the spirit of the rigid-band model (discussed in rigid-shift section below) and doping merely shifts down the E_F. The persistence of CuO_2 properties is also substantiated by the same anti-ferromagnetic ordering in CuO_2 in the whole phase diagram in LSCO [48].

Equipped with this modulation doping mechanism, we can re-examine the experiments of the interface superconductivity between insulating La_2CuO_4 (I-LCO) and metallic $La_{1.55}Sr_{0.45}CuO_4$ or $La_{1.64}Sr_{0.36}CuO_4$ (M-LSCO) [14, 15]. Typical values for T_c at the mid-point of the resistive transitions are $T_C \approx 15$ K in I–M and $T_C \approx 30$ K in M–I structures. Replacing a small amount (3%) of Cu by Zn in one single layer of M–I structure reduces T_c and a pronounced depression of T_c occurs when the Zn dopant atoms are placed in the $N = 2$ layer (i.e. the second CuO_2 plane above the LSCO–LCO interface), showing that this interface high-temperature superconductivity occurs within a single CuO_2 plane [15].

For δ-doping of LCO structure, the T_c is highly space-dependent and the Zn tomography identifies the plane which is two CuO_2 layers away from the interface as the main source of high-T_c superconductivity of the downward side [49]. Note that δ-doping, two-dimensional doping or modulation doping means one or a few complete unit cells of a doped material in a matrix of the same but undoped material. In contrast to the agreement between the Sr and holes profile at the upward side interface where superconductivity could be explained by homogeneous doping [49], the higher holes value compared with Sr concentration at the interface facing substrate could only be understood by charge accumulation in our band bending model in which one side of the interface is reduced to only one atomic layer (LCO).

Thus, based on interface superconductivity between I-LCO and M-$La_{1.55}Sr_{0.45}CuO_4$ or $La_{1.64}Sr_{0.36}CuO_4$ [14, 15] and δ-doping of LCO [49], we can safely infer that the band bending occurs between CuO_2 single layer and reservoirs in cuprates, providing the superfluid density for superconductivity.

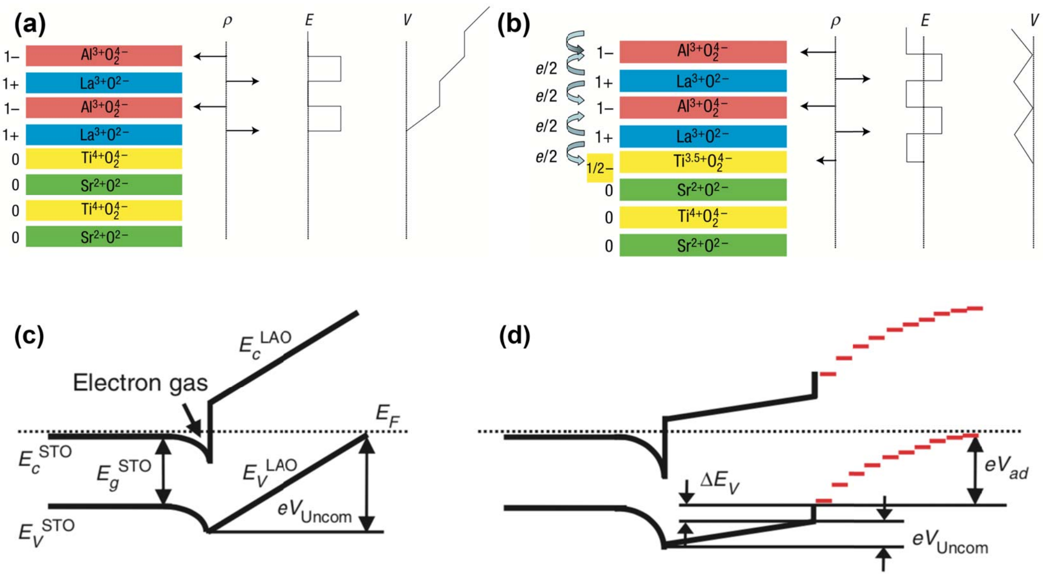

Figure 4. The polar catastrophe illustrated for atomically abrupt LAO/STO interfaces. (a) The unreconstructed interface has neutral planes in STO, but the LAO has alternating net charges. For AlO_2/LaO/TiO_2 interface, a positive electric field (E) and an electric potential (V) that diverges with thickness are formed. (b) The divergence catastrophe can be avoided if half of electrons are added to the last Ti layer. This produces an interface dipole that causes the electric filed to oscillate about zero and the potential remains finite [54]. (c) Idealized surface. Electrons transfer from the valence band of the LAO surface (E_V^{LAO}) to the conduction band of the STO (E_C^{STO}), near the interface. eV_{uncom} (the shifted band energy) roughly equals to E_g^{LAO}. (d) Surface with aligned polar adsorbates. Electrons transfer from the surface adsorbates to E_C^{STO} near the interface. The built-in potential across the adsorbates (V_{ad}) effectively reduces V_{uncom} across the LAO layer [55].

2.3. *Band bending in LAO/STO*

The finding of a conducting layer at the interface between the wide band gap perovskite insulators LAO and STO [31] with high mobility and superconductivity [50, 51] has triggered much attention. Its hole counterpart has been recently observed in the p-type interface [52]. It is found that LAO/STO and cuprates share many characters in common such as dome, pseudogap behavior [51] and the increase of superconducting thickness when approaching the overdoped regime [25, 53]. The most important common feature is the polar nature, leading to the tilted band structure in LAO or cuprates and the so called “polar catastrophe” [54]. Polar catastrophe means the divergent built-in electrostatic potential resulting from the alternate stacking of positively and negatively charged layers. Take n-type interface for example, to avoid the polar discontinuity, half of electrons are transferred from positively charged LaO at the interface to the lower TiO_2 and another half is transferred to the adjacent negatively charged AlO_2 [54] (Figures 4(a) and (b)), providing a complementary source of 2DEL apart from band bending.

The slope of LAO’s band can be tuned by surface adsorbates as shown in Figures 4(c) and (d) [55] as well as by surface ferroelectric polarization [56]. Note that LAO’s band shifts upwards more slowly with surface polar adsorbates. The interface carrier density can be deduced as $\sigma_{\mathrm{inter}} = (\sigma_0/2) - (\epsilon_{\mathrm{LAO}}/e \cdot d_{\mathrm{LAO}}) V_{\mathrm{uncom}}$, where $\sigma_0/2$ is the transferred electron due to the polar catastrophe, d_{LAO} is the LAO thickness and V_{uncom} is the upward shift of LAO's band [55]. Thus the interface carrier density would increase with the slowing-down slope. This equation could explain the increase in $\Delta(1/R_{\mathrm{sheet}})$ observed after surface adsorption using polar solvents, independent of their aprotic or protic character [55]. The extreme situation for surface adsorption is metallic surface doping which should cancel out the built-in potential completely and σ_{inter} approaches $\sigma_0/2$. According to density functional theory calculations, this is indeed the case for Na and Ti capping layers while Ag and Cu leave a little built-in potential and Au enhances the built-in potential due to Au's large work function [57]. In 2018, a possible superconducting state was observed near Ti and Al electrodes [58].

Besides, the slope of LAO's band as well as the carrier density can be tuned by δ-doping. In LAO/STO, δ-doping of a fraction of monolayer of $LaMnO_3$ (LMO) at the interface LAO will decrease the carrier density between the heterosructure and slow down the slope of LAO's band simultaneously [59]. Due to mixed-valent character of the Mn ion between Mn^{3+} and Mn^{4+} states, electrons are transferred from $Mn_{\delta}Al_{1-\delta}O_2^-$ to the LaO layer, opposite to the charge transfer direction resulting from the polar catastrophe. Thus, the transferred electrons due to polar catastrophe is reduced significantly. The concomitant decrease of V_{uncom} is small compared to the loss of transferred electrons, so the carrier density decreases.

LAO/STO provides a paradigmatic example for polar/nonpolar interface and similar polar/nonpolar oxide heterostructures are $LaTiO_3$/STO [60], $KTaO_3$/STO [61], $LaVO_3$/STO [62], LMO/$SrMnO_3$ [63], $KTaO_3$/EuO [64], $KTaO_3(111)$/$LaTiO_3(111)$ [65] and $KTaO_3(111)$/EuO [65]. All the arguments above go for these systems as well. Note that superconductivity found for $KTaO_3(111)$/$LaTiO_3(111)$ and $KTaO_3(111)$/EuO is strongly dependent on carrier density [65]. Besides, the absence of superconductivity in $LaTiO_3(100)$ related interfaces indicates the influence of larger polarity discontinuity in $LaTiO_3(111)$ related interfaces.

The polar/nonpolar interfaces represented by LAO/STO are important in the sense that layers in cuprates are polar too, especially CuO_2. Besides, LAO/STO resembles cuprates in that it also has a dome and pseudogap behavior [51] and superconducting thickness increases when approaching the overdoped regime [25, 53]. The ability of tuning by surface adsorbates, ferroelectric polarization and δ-doping opens a new field of remote doping for polar/nonpolar interfaces.

3. Rigid shift

As a natural deduction of band bending, here, the band shift upon doping in different interface superconductors is discussed as well as the Fermi surface geometry. However, people prefer strong correlations to the rigid shift mainly for three reasons. First, in-gap states are formed during doping as observed by scanning tunneling microscopy (STM) [66] and ARPES [67]. Second, the detection of a d-wave like pseudogap emphasizes the inadequacy of a rigid-band description for the electronic structure of the high-T_c superconductors [68]. Third, the chemical potential is pinned in underdoped region for LSCO [69] with lower Hubbard band (LHB) stays away from E_F (at -0.5 eV) [67]. However, we propose that the strong correlations form the basis band structures of either iron-based superconductors or cuprates and doping merely changes the E_F. As shown later, there have been many observations and hints of rigid shift in both systems.

For iron-based superconductors, rigid band shift has been reported in $Ba(Fe_{1.94}Co_{0.06})_2As_2$ [70] with a shift of 14 meV and in bulk FeSe [71]. Besides, Fermi surface evolution from hole pocket at Γ and electron pocket at M to electron pocket at M in both bulk FeSe [36] and FeSe/STO [35, 72] confirms the physical picture in Figure 5(a). Also the rigid band shift comes from the fact that low T_c undoped bulk materials are compensated semimetals [73] while electron doped materials have no hole Fermi pocket [2–4, 34, 74–76]. Note that $(Tl,Rb)_xFe_{2-y}Se_2$ has a shorter distance (smaller than 50 meV) between the two electron pockets at Γ and M compared to FeSe [2]. This

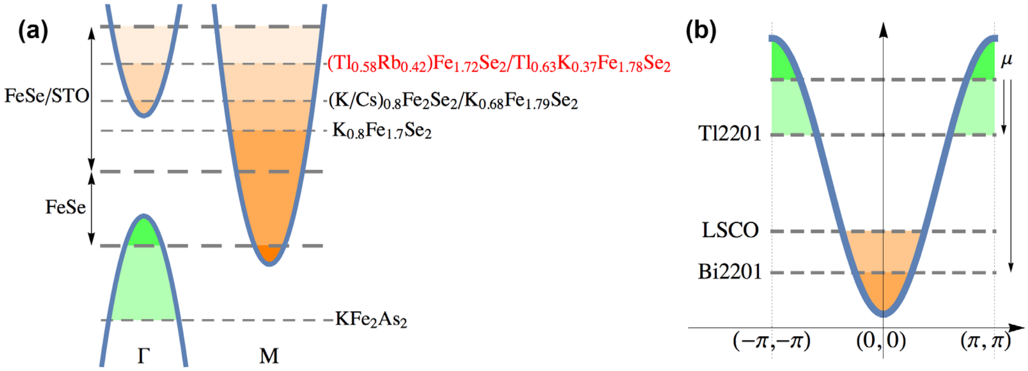

Figure 5. (a) A simple sketch of the E–k dispersion and chemical potential's rigid shift in FeSe and FeAs family. For extremely electron doped FeSe, it harbors electron pockets at both Γ and M [72]. $Tl_{0.58}Rb_{0.42}Fe_{1.72}Se_2$ [75] and $Tl_{0.63}K_{0.37}Fe_{1.78}Se_2$ [78] locate near this doping level. $(K/Cs)_{0.8}Fe_2Se_2$ ($T_C \sim 30$ K) [76] and $K_{0.68}Fe_{1.79}Se_2$ ($T_C \sim 32$ K) [79] are beneath this doping level and $K_{0.8}Fe_{1.7}Se_2$ ($T_C \sim 30$ K) locates further below [80]. For extremely hole doped KFe_2As_2, it has only the hole pocket at Γ [81]. (b) The chemical potential shift for Tl2201, Bi2201 and LSCO with the same E–k dispersion from CuO_2 [82] along the high symmetry line $(-\pi,-\pi)-(\pi,\pi)$.

may be the result of Tl's electrons involved in the bands or the consequence of higher nematicity in bulk FeSe [77], discarding $(Tl,Rb)_xFe_{2-y}Se_2$ as one member in the rigid shift family of FeSe.

Secondly, the rigid E–k dispersion was also reported in some cuprate compounds. The E–k dispersion is not distorted with varying hole-concentration of cuprates at least from underdoped to the overdoped near optimal doped conditions with the ARPES measurements of $(Bi,Pb)_2(Sr,La)_2\,CuO_{6+\delta}$ (Bi2201) [27]. Earlier study shows that the band dispersion of Bi2201 is also fairly rigid in the overdoped range [83]. For extremely overdoped situation, the quantum well is destroyed [25]. Further, the rigid shift of chemical potential with doping has been verified in $Ca_{2-x}Na_xCuO_2Cl_2$ (Na–CCOC) [84, 85] via a new method based on the valence orbital of oxygen. Other verified systems are Bi2212 [86] and Bi2201 [83, 87]. Besides, the Fermi surface changing from hole-like pocket at X to electron-like pocket at Γ [88] is confirmed to be the rigid shift of the chemical potential in LSCO [87]. This Fermi surface evolution is universal for CuO_2 and tetragonal CuO (T-CuO) [82] because the two systems share the same CuO_2 structures. The Fermi surface reconstruction of electron-doped cuprates is complicated due to the (π,π) shift of the AFM correlations [89], in which the conduction band is formed by the original UHB along with the shifted UHB with the AFM order parameter $\langle\varphi_\alpha\rangle \neq 0$, i.e. the gap is formed at the hotspots. The $x = 0.04$ Fermi surface can be viewed as the electron doped Fermi surface with the shifted UHB [89]. With Ce doping, $Nd_{2-x}Ce_xCuO_{4\pm\delta}$ is gradually electron doped [90] and the AFM disappears at $x = 0.15$. The Fermi surface evolution from electron pocket at $(\pi,0)$ to hole pocket at (π,π) [91] can be viewed as doping from the shifted UHB to the unshifted UHB.

Finally, we would point out that the same doping level corresponds to different chemical potential levels for different materials. For example, among the three compounds (Bi2212, Bi2201 and LSCO), the three cuprates have maximum T_c at $x = 0.15$ while they correspond to two different Fermi surface areas, indicating two different chemical potentials since the Fermi surface area is controlled by the rigid shift of chemical potential [27]. Another evidence is the large hole pocket rather than the Fermi surface reconstruction (as in overdoped Bi2201 [27] and LSCO [87, 88]) in overdoped $Tl_2Ba_2CuO_{6+\delta}$ (Tl2201) [92] which is depicted in Figure 5(b). The inconsistent chemical potential also exists in electron-doped cuprates since optimal-doped $Nd_{2-x}Ce_xCuO_{4\pm\delta}$ has a large Fermi surface centered at (π,π) [91] while a reconstructed Fermi surface is favored for the optimal-doped $Sm_{2-x}Ce_xCuO_{4+\delta}$ [93].

The above conclusion has two deductions. First, the Fermi surface geometry has no effect on superconductivity. Both non-superconducting $Ba(Fe_{1-x}Co_x)As_2$ beyond $x = 0.2$ [94] and superconducting $Tl_{0.58}Rb_{0.42}Fe_{1.72}Se_2$ [75] have electron pockets at Γ (Figure 5(a)). Besides, the superfluid density is much larger than the electron density expected from ARPES of the excess electron count [42], indicating that the electron source for superconductivity is not from FeSe's electron pockets. According to the modulation doping scenario, superconductivity is achieved once the carriers in the quantum well exceed a certain concentration [25]. In this vein, the Fermi level outside the quantum well which determines the size and the shape of the Fermi surface will not affect the superconductivity. Another deduction is the asymmetry of electron-dome and hole-dome in the phase diagram due to the different chemical potentials for $x = 0$, which determines the maximum quantum well carriers, in different materials.

It is worth pointing out the rigid shift with temperature as follows. This has been observed in iron-based superconductors by ARPES in FeSe with ∼25 meV upwards shift from 100 K to 300 K [95], in $Ba(Fe_{1-x}Ru_x)_2As_2$ with ∼35 meV upwards shift from 50 K to 300 K [96], in 0.08 Co doped $BaFe_2As_2$ with ∼30 meV upwards shift from 0 K to 300 K [97] and 0.3 Co doped $BaFe_2As_2$ with ∼30 meV downwards shift from 0 K to 300 K [97]. The shift direction is determined by the essence of the pockets as shown in Figure 6(a–d). For electron pockets, the rectangle area between the conductance band and the E_F is occupied at zero temperature. Once the temperature increases, the occupation of electron extends beyond the E_F (the grey line in Figure 6(a)). Compared to zero temperature, the unoccupied area is much smaller than the occupied area. To keep the carriers conserved at high temperature, the unoccupied and occupied area should be balanced, thus the E_F should shift downwards to E_F' (Figure 6(c)). As for hole pockets, the E_F shifts in the opposite way. Assuming the same shift value for cuprates and combining with the fact of the dominating hole pockets, many phenomena could be explained. First is the linear decrease of the gap for about 30 meV near anti-nodal direction [68]. Second, the rigid shift could also be used to understand the linear decrease of the Fermi arc observed in Bi2212 [98].

4. Electron–phonon coupling

In addition to the band alignment and rigid shift contributing to the interface superconductivity of 1UC FeSe/STO, other interfacial effects such as EPC is involved for enhancing T_c in this system as well [11, 99]. Subsequent ARPES experiments reveal that each primary electronic band of 1UC FeSe/STO has a fainter replica band offset by 100 meV [9], as shown in Figures 7(a) and (b). Such replicas were absent in FeSe films of two layers or thicker, pointing to an interfacial origin of these features. Similar phenomenology was observed by Peng *et al.* in 1UC FeSe/$BaTiO_3$ (BTO) [74]. The authors attributed the replica bands to bosonic shake-off, and identified the boson with an optical O phonon band calculated for bulk STO [100]. Recently, Li *et al.*, however, argued that the replica bands are nothing but the result of the strong coupling of external propagating electrons instead of Fe electrons to Fuchs–Kliewer (F–K) surface phonons in ionic materials [101]. Then Song *et al.* rules out this extrinsic origin of the replica bands by O isotope substitution [102]. Many studies were performed to argue the phonon roles in superconductivity of 1UC FeSe/STO.

4.1. *The unaffected phonons in the FeSe films*

The 10 meV and 20 meV phonons were found to rest in the FeSe films themselves [104, 105]. However, the indifference of the dispersion and line widths profiles of phonons, which can reflect

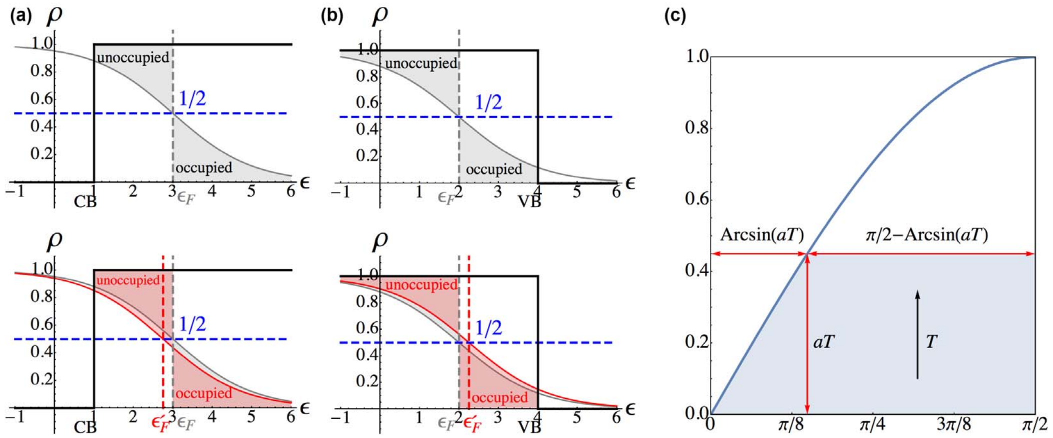

Figure 6. (a) The Fermi distribution for electron pockets for unshifted E_F (upper panel) and shifted E_F (lower panel) at high temperatures. (b) The Fermi distribution for hole pockets for unshifted E_F (upper panel) and shifted E_F (lower panel) at high temperatures. The red areas marks the unoccupied area and the occupied area compared with zero temperature distribution. (c) Sketch of the temperature dependent Fermi arc.

the strength of mode-specific EPC [106], for various thickness films demonstrate that the EPC from FeSe phonons is not directly related to the interfacial T_c enhancement. The unchanged surface Debye temperature for various thicknesses measured by LEED [103], which falls in the range of the Debye temperature of bulk FeSe [107, 108], is another sign of FeSe phonons' irrelevance to thickness.

4.2. *The interacting phonons in STO*

As mentioned above, the phonon role in STO is first awaked from the replica bands (100 meV) observed by ARPES [5, 109]. Theorists found that the 99 meV mode and 53 meV ferroelectric phonon mode deal with the interfacial superconductivity [110]. Moreover, the proximity of STO's ferroelectric transition temperature and 1UC FeSe/STO's superconducting T_c imply a possible correlation between the substrate lattice and enhancement of superconductivity at the interface [111]. Later, the penetration of the STO F–K phonons (α and β as shown in Figure 7(c)) into FeSe film is revealed by HREELS [112]. The penetrated F–K phonon mode decays exponentially with FeSe thickness, which matches well with the observed exponential decay of the superconducting gap [112]. Then it is found that surface F–K phonon modes of the substrate are temperature dependent (Figure 7(e)) [103], which is a sign for EPC. The intensity of the overtone $\beta + A_{1g}/B_{1g}$, which is the new energy loss mode caused by the involvement of Se- and Fe-derived phonons A_{1g} and B_{1g}, increases with increasing temperature (Figure 7(d)). Due to the anharmonic phonon–phonon interaction, which leads to the decay of F–K modes into other low-energy FeSe phonons, the energy of α mode softens a lot on 1UC FeSe/STO surface with the increasing temperature (Figure 7(e)). The new energy loss mode $\beta + A_{1g}/B_{1g}$ and the soften of α mode contribute to the difference caused by FeSe deposition for temperature dependent line profile of the energy loss spectra, which is another sign for EPC. The third remark of EPC is that the linewidths (Γ_{ep}) of F–K phonon modes related to 1UC FeSe/STO are larger compared to those of clean STO(001) [103]. Thicker films have broader F–K phonons since all the electrons in FeSe films will interact with the phonons from substrate. However, the exponential decay of the electric field weakens the contribution from further layers [112]. Recently, electrons are disclosed to

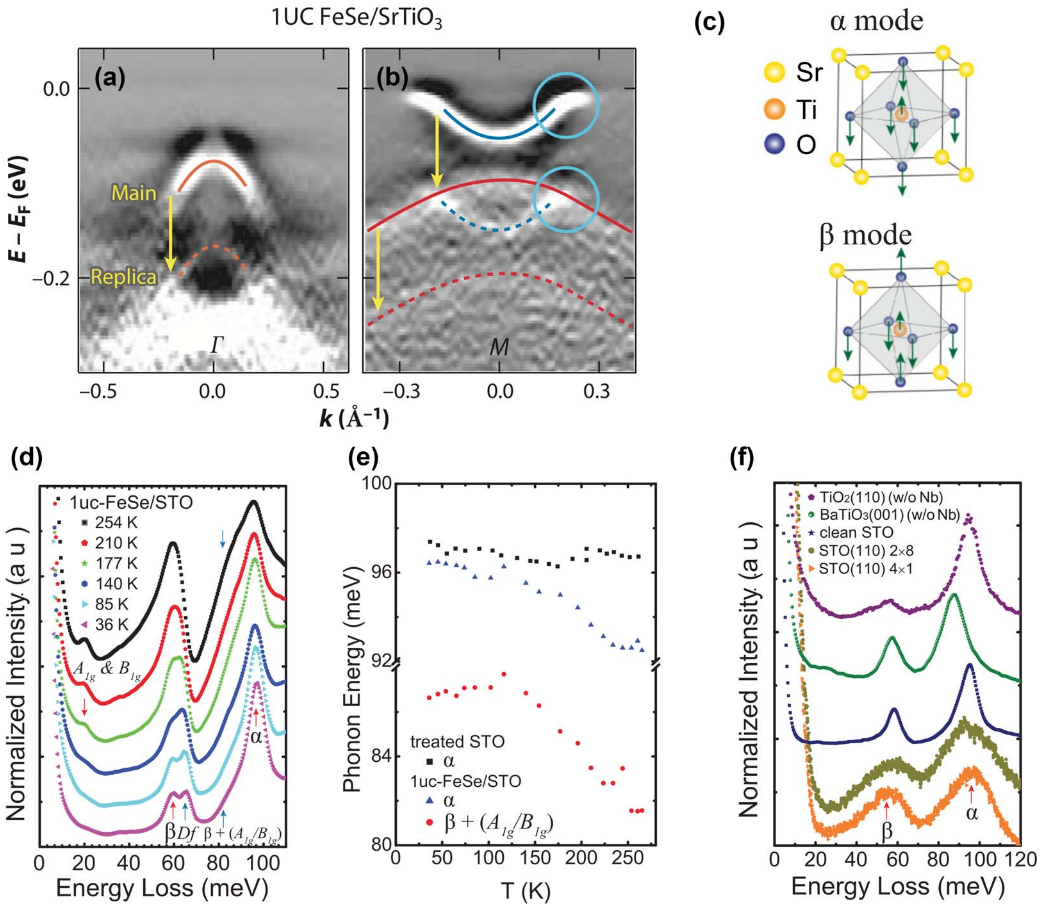

Figure 7. (a, b) ARPES high-symmetry cuts of 1UC FeSe/STO showing primary electronic bands (solid line overlays) and corresponding replica bands (dashed line overlays)—fainter duplicates of the primary bands, shifted down by 100 meV (yellow arrows). These replica features suggest a $\mathbf{q} \sim 0$ coupling to STO phonon mode. The blue circles highlight the duplication of a back-bending dispersion in the primary band as a superconducting gap opens near the E_F [9]. (c) Illustration of ionic vibrations of Fuchs–Kliewer (F–K) phonons in STO [103]. (d) Temperature-dependent energy distribution curves (EDCs) of 1UC FeSe/STO at $\bar{\Gamma}$ point [103]. (e) Plot of energies of several modes as a function of temperature for treated STO and 1UC FeSe/STO at $\bar{\Gamma}$ point [103]. (f) Energy loss spectra at $\bar{\Gamma}$ point of several typical oxide surfaces: rutile $TiO_2(110)$ (without Nb), BTO (without Nb), STO(110) 2×8, STO(110) 4×1, and clean STO, all at room temperature [103].

be dressed by the strongly polarized lattice distortions in STO, forming the interfacial dynamical polarons non-adiabatically, which propagate as polaronic plasmon mode and are correlated with the surface phonon modes (mainly α) of STO [113]. Aside from these results, the most obvious sustainment for EPC comes from the lock-in measurements by ARPES and X-ray diffraction [114], who monitored the ratios of the band energy shift as well as the synchronized atomic displacement at the Brillouin Zone center.

It is worthy pointing out the universality of T_c enhancement when 1UC FeSe grown on various oxide substrates with high energy bonds like Ti–O bonds or other. Such substrates include BTO(001) [74], STO(110) [115, 116], anatase $TiO_2(001)$ [117], rutile $TiO_2(001)$ [118] and $GaO_{2-\delta}$ [119]. High-energy F–K phonons present also in a variety of oxide substrates with similar energies as shown in Figure 7(f). Besides, UPS revealed the dramatic enhancement of the Ti–O bonding peak, indicating the enhanced EPC with annealing [40]. Thus we can safely conclude that polar TiO_2 bonds are relevant to the F–K phonons.

4.3. *The antiferromagnetic (AFM) correlations*

It has been widely accepted that magnetic correlation or spin fluctuation is critical in nonmagnetic FeSe bulk [120, 121]. Under pressure, μSR and magnetization measurement highlight that a static AFM order coexists with the superconductivity [16]. Having comprehended the high mangetic susceptibility in iron-based superconductors [16], the deficiency of EPC to overcome the destructive effects of strong spin fluctuations [17, 18], the AFM order in epitaxial FeSe films on STO [122, 123], the weakened EPC due to electronic fluctuations screening [124] and inadequacy of prediction about high T_c by EPC [19, 20], most theorists are well in a position to argue for the superconductivity mediated by AFM spin fluctuations. They propose an extended s-wave pairing with a π phase shift between hole and electron Fermi surfaces [17]. In addition, for FeSe, Benfatto *et al.* [18] offered an orbital-selective spin fluctuations scenario which incorporates the anisotropic pairing interaction mediated by nematic spin fluctuations to explain the large anisotropy of the electronic properties. In this scenario, the nematic spin fluctuations have the orbital ordering induced by the nematic shrinking of the Fermi surface pockets below the nematic transition. Both large-q spin fluctuations (sign reversal on different Fermi surfaces) and small-q EPC (same sign on the same pockets) are believed to be the sources of the Cooper pairing cooperatively [11]. What's more, it has been substantiated that the substrate enhances the T_c in allowing AFM ground state of FeSe which opens EPC channels within the monolayer [104]. STO induced AFM ground states in thin films are also observed in other thin films like LAO [125] and $LaFeO_3$ [126].

Apart from mediating the superconductivity, FeSe's AFM correlations strengthen EPC as well. Previous calculations found a much stronger EPC in the magnetic phase than in the nonmagnetic phase [127]. Besides, ARPES results are closely resembled to the FeSe with an AFM checkerboard spin pattern for FeSe/STO [128, 129]. The band splitting associated with an AFM order or instability was observed in FeSe/STO by ARPES [121]. Further, the AFM ground state for the undoped FeSe/STO by magnetic exchange bias effect was discovered directly for the first time that the AFM order disappears after electron doping [123]. Calculations manifest the indispensable role of FeSe's AFM correlation in rendering quantitatively the experimental phonon dispersion in the ultrathin FeSe films [103].

From above discussion, the interface provides charge transfer from the substrate. What's more, the substrate is the source of the strong EPC by providing phonons [5, 109], holding FeSe near its structural and magnetic phase transitions [104] as well as allowing AFM ground state FeSe which opens EPC channels within the monolayer [103, 104]. This spatial dichotomy between Cooper pairs which reside in the conducting 2DEG and the source of pairing which originates from the substrate is also proposed in LAO/STO [53]. As for cuprates, there are signatures for EPC such as the delay of photoinduced response below T_c in time-resolved ARPES [130], kinks in the real part of self-energy, kinks in dispersion at both nodal and antinodal directions and peak-dip-hump feature [131], indicating the existence of 36 meV B_{1g} oxygen bond-buckling phonon mode, 60~90 meV full and half-breathing mode associated with in-plane O vibrations and around 70 meV apical O vibrations mode [131]. Further, the spin fluctuations are recently challenged by the acoustic plasmon [132], which are believed to mediate substantial superconductivity in electron doped cuprates, formed by the layered electron gas model with interplanar Coulomb interactions. Inspired by studies in FeSe/STO and LAO/STO, we may speculate similar roles of phonons in cuprates. However, the isotope experiments with O exchange in cuprates are complicated by apical and chain O atoms [23] while only plane O atoms dominate in superconductivity. Thus smoking-gun site-selective isotope experiments are expected to reveal the pairing mechanism in cuprates.

5. Summary

Interface superconductivity is currently a subject of fast-paced research due to its potential in superconducting technology application as well as fundamental scientific interest in understanding high-T_c superconductivity. Within the past decade, various interfaces with superconductivity have been discovered. FeSe/STO, LCO/LSCO, LAO/STO are three representative examples for polar/nonpolar interfaces. Besides, iron-based superconductors and cuprates are believed to consist of iron-based layers/CuO_2 as well as non-superconducting layers, another kind of "interface system". We review these systems with ideas of band bending and charge transfer borrowed from semiconductors. Among them, FeSe/STO exemplifies a dramatic interface effect in high-temperature superconductivity. FeSe/STO's high-T_c supports the existence of charge transfer due to band bending and the gluing role of EPC and AFM correlations. LCO/LSCO confirms the band bending mechanism in cuprates and validates the E_F definition in the limit of single layer. As a natural deduction of band bending, the rigid shift is discussed in the context of iron-based superconductors and cuprates. As for the polar/nonpolar interface LAO/STO, it points out one important aspect of polar CuO_2 in cuprates and inspires us with new ways to remotely dope the interface. Equipped with this unified physical picture, more interface superconductors would be discovered accordingly.

Acknowledgements

The work was financially supported by the Ministry of Science and Technology of China, the Natural Science Foundation of China, and in part by the Beijing Advanced Innovation Center for Future Chip (ICFC).

References

[1] Q.-Y. Wang, Z. Li, W.-H. Zhang, Z.-C. Zhang, J.-S. Zhang, W. Li, H. Ding, Y.-B. Ou, P. Deng, K. Chang *et al.*, "Interface-induced high-temperature superconductivity in single unit-cell FeSe films on $SrTiO_3$", *Chin. Phys. Lett.* **29** (2012), no. 3, article no. 037402.

[2] D.-F. Liu, W.-H. Zhang, D.-X. Mou, J.-F. He, Y.-B. Ou, Q.-Y. Wang, Z. Li, L.-L. Wang, L. Zhao, S.-L. He *et al.*, "Electronic origin of high-temperature superconductivity in single-layer FeSe superconductor", *Nat. Commun.* **3** (2012), article no. 931.

[3] S.-L. He, J.-F. He, W.-H. Zhang, L. Zhao, D.-F. Liu, X. Liu, D.-X. Mou, Y.-B. Ou, Q.-Y. Wang, Z. Li *et al.*, "Phase diagram and electronic indication of high-temperature superconductivity at 65 K in single-layer FeSe films", *Nat. Mater.* **12** (2013), no. 7, p. 605-610.

[4] S.-Y. Tan, Y. Zhang, M. Xia, Z.-R. Ye, F. Chen, X. Xie, R. Peng, D.-F. Xu, Q. Fan, H.-C. Xu *et al.*, "Interface-induced superconductivity and strain-dependent spin density waves in FeSe/$SrTiO_3$ thin films", *Nat. Mater.* **12** (2013), no. 7, p. 634-640.

[5] J. J. Lee, F. T. Schmitt, R. G. Moore, S. Johnston, Y.-T. Cui, W. Li, M. Yi, Z. K. Liu, M. Hashimoto, Y. Zhang *et al.*, "Interfacial mode coupling as the origin of the enhancement of T_c in FeSe films on $SrTiO_3$", *Nature* **515** (2014), no. 7526, p. 245-248.

[6] L. Z. Deng, B. Lv, Z. Wu, Y. Y. Xue, W. H. Zhang, F. S. Li, L. L. Wang, X. C. Ma, Q. K. Xue, C. W. Chu, "Meissner and mesoscopic superconducting states in 1–4 unit-cell FeSe films", *Phys. Rev. B* **90** (2014), no. 21, article no. 214513.

[7] J.-F. Ge, Z.-L. Liu, C.-H. Liu, C.-L. Gao, D. Qian, Q.-K. Xue, Y. Liu, J.-. Jia, "Superconductivity above 100 K in single-layer FeSe films on doped $SrTiO_3$", *Nat. Mater.* **14** (2015), no. 3, p. 285-289.

[8] A. K. Pedersen, S. Ichinokura, T. Tanaka, R. Shimizu, T. Hitosugi, T. Hirahara, "Interfacial superconductivity in FeSe ultrathin films on $SrTiO_3$ probed by *in situ* independently driven four-point-probe measurements", *Phys. Rev. Lett.* **124** (2020), article no. 227002.

[9] D. Huang, J. E. Hoffman, "Monolayer FeSe on $SrTiO_3$", *Annu. Rev. Condens. Matter Phys.* **8** (2017), p. 311-336.

[10] Z. Wang, C. Liu, Y. Liu, J. Wang, "High-temperature superconductivity in one-unit-cell FeSe films", *J. Phys.: Condens. Matter* **29** (2017), no. 15, article no. 153001.

[11] D.-H. Lee, "Routes to high-temperature superconductivity: A lesson from FeSe/$SrTiO_3$", *Annu. Rev. Condens. Matter Phys.* **9** (2018), p. 261-282.

[12] P. A. Lee, N. Nagaosa, X.-G. Wen, "Doping a Mott insulator: physics of high-temperature superconductivity", *Rev. Mod. Phys.* **78** (2006), p. 17-85.

[13] I. Božović, C. Ahn, "A new frontier for superconductivity", *Nat. Phys.* **10** (2014), no. 12, p. 892-895.

[14] A. Gozar, G. Logvenov, L. F. Kourkoutis, A. T. Bollinger, L. A. Giannuzzi, D. A. Muller, I. Božović, "High-temperature interface superconductivity between metallic and insulating copper oxides", *Nature* **455** (2008), no. 7214, p. 782-785.

[15] G. Logvenov, A. Gozar, I. Božović, "High-temperature superconductivity in a single copper–oxygen plane", *Science* **326** (2009), no. 5953, p. 699-702.

[16] M. Bendele, A. Amato, K. Conder, M. Elender, H. Keller, H.-H. Klauss, H. Luetkens, E. Pomjakushina, A. Raselli, R. Khasanov, "Pressure induced static magnetic order in superconducting $FeSe_{1-x}$", *Phys. Rev. Lett.* **104** (2010), article no. 087003.

[17] I. I. Mazin, D. J. Singh, M. D. Johannes, M. H. Du, "Unconventional superconductivity with a sign reversal in the order parameter of $LaFeAsO_{1-x}F_x$", *Phys. Rev. Lett.* **101** (2008), article no. 057003.

[18] L. Benfatto, B. Valenzuela, L. Fanfarillo, "Nematic pairing from orbital-selective spin fluctuations in FeSe", *NPJ Quantum Mater.* **3** (2018), no. 1, article no. 56.

[19] B. Li, Z. W. Xing, G. Q. Huang, D. Y. Xing, "Electron–phonon coupling enhanced by the FeSe/$SrTiO_3$ interface", *J. Appl. Phys.* **115** (2014), no. 19, article no. 193907.

[20] Y. Wang, A. Linscheid, T. Berlijn, S. Johnston, "Ab initio study of cross-interface electron–phonon couplings in FeSe thin films on $SrTiO_3$ and $BaTiO_3$", *Phys. Rev. B* **93** (2016), article no. 134513.

[21] T. P. Devereaux, A. Virosztek, A. Zawadowski, "Neutron scattering and the B_{1g} phonon in the cuprates", *Phys. Rev. B* **59** (1999), p. 14618-14623.

[22] Z. An-Min, Z. Qing-Ming, "Electron–phonon coupling in cuprate and iron-based superconductors revealed by Raman scattering", *Chin. Phys. B* **22** (2013), no. 8, article no. 087103.

[23] H. Keller, A. Bussmann-Holder, K. A. Müller, "Jahn–Teller physics and high-T_c superconductivity", *Mater. Today* **11** (2008), no. 9, p. 38-46.

[24] L.-L. Wang, X.-C. Ma, Q.-K. Xue, "Interface high-temperature superconductivity", *Supercond. Sci. Technol.* **29** (2016), no. 12, article no. 123001.

[25] Y. Zhong, Y. Wang, S. Han, Y. F. Lv, W. L. Wang, D. Zhang, H. Ding, Y. M. Zhang, L. L. Wang, K. He *et al.*, "Nodeless pairing in superconducting copper-oxide monolayer films on $Bi_2Sr_2CaCu_2O_{8+\delta}$", *Sci. Bull.* **61** (2016), no. 16, p. 1239-1247.

[26] Y.-M. Zhang, J.-Q. Fan, W. L. Wang, D. Zhang, L. L. Wang, W. Li, K. He, C. L. Song, X. C. Ma, Q. K. Xue, "Observation of interface superconductivity in a $SnSe_2$/epitaxial graphene van der Waals heterostructure", *Phys. Rev. B* **98** (2018), article no. 220508.

[27] T. Kondo, T. Takeuchi, T. Yokoya, S. Tsuda, S. Shin, U. Mizutani, "Hole-concentration dependence of band structure in $(Bi,Pb)_2(Sr,La)_2CuO_{6+\delta}$ determined by the angle-resolved photoemission spectroscopy", *J. Electron. Spectros. Relat. Phenomena* **137** (2004), p. 663-668.

[28] C. C. Tsuei, J. R. Kirtley, "Pairing symmetry in cuprate superconductors", *Rev. Mod. Phys.* **72** (2000), p. 969-1016.

[29] H. Won, K. Maki, "d-wave superconductor as a model of high-T_c superconductors", *Phys. Rev. B* **49** (1994), p. 1397-1402.

[30] Y.-Y. Zhu, M.-H. Liao, Q.-H. Zhang, H.-Y. Xie, F.-Q. Meng, Y.-W. Liu, Z.-H. Bai, S.-H. Ji, J. Zhang, K.-L. Jiang *et al.*, "Presence of s-wave pairing in Josephson junctions made of twisted ultrathin $Bi_2Sr_2CaCuO_{8+\delta}$ flakes", *Phys. Rev. X* **11** (2021), article no. 031011.

[31] A. Ohtomo, H. Hwang, "A high mobility electron gas at the $LaAlO_3$/$SrTiO_3$ heterointerface", *Nature* **427** (2004), no. 6973, p. 423-426.

[32] B. Lei, J. H. Cui, Z. J. Xiang, C. Shang, N. Z. Wang, G. J. Ye, X. G. Luo, T. Wu, Z. Sun, X. H. Chen, "Evolution of high-temperature superconductivity from a low-T_c phase tuned by carrier concentration in FeSe thin flakes", *Phys. Rev. Lett.* **116** (2016), article no. 077002.

[33] X. F. Lu, N. Z. Wang, H. Wu, Y. P. Wu, D. Zhao, X. Z. Zeng, X. G. Luo, T. Wu, W. Bao, G. H. Zhang *et al.*, "Coexistence of superconductivity and antiferromagnetism in $(Li_{0.8}Fe_{0.2})$OHFeSe", *Nat. Mater.* **14** (2015), no. 3, p. 325-329.

[34] L. Zhao, A. J. Liang, D. N. Yuan, Y. Hu, D. F. Liu, J. W. Huang, S. L. He, B. Shen, Y. Xu, X. Liu *et al.*, "Common

electronic origin of superconductivity in (Li,Fe)OHFeSe bulk superconductor and single-layer FeSe/$SrTiO_3$ films", *Nat. Commun.* **7** (2016), article no. 10608.

[35] Y. Miyata, K. Nakayama, K. Sugawara, T. Sato, T. Takahashi, "High-temperature superconductivity in potassium-coated multilayer FeSe thin films", *Nat. Mater.* **14** (2015), no. 8, p. 775-779.

[36] C. P. Wen, H. C. Xu, C. Chen, Z. C. Huang, X. Lou, Y. J. Pu, Q. Song, B. P. Xie, M. Abdel-Hafiez, D. Chareev *et al.*, "Anomalous correlation effects and unique phase diagram of electron-doped FeSe revealed by photoemission spectroscopy", *Nat. Commun.* **7** (2016), article no. 10840.

[37] J. Seo, B. Kim, B. S. Kim, J. Jeong, J. Ok, J. S. Kim, J. Denlinger, S.-K. Mo, C. Kim, Y. K. Kim, "Superconductivity below 20 K in heavily electron-doped surface layer of FeSe bulk crystal", *Nat. Commun.* **7** (2016), article no. 11116.

[38] J. Stahl, D. Johrendt, "$FeSe(en)_{0.3}$-separated FeSe layers with stripe-type crystal structure by intercalation of neutral spacer molecules", https://arxiv.org/abs/1706.00314, 2017.

[39] M. K. Xu, X. Q. Song, H. Wang, "Substrate and band bending effects on monolayer FeSe on $SrTiO_3$(001)", *Phys. Chem. Chem. Phys.* **19** (2017), no. 11, p. 7964-7970.

[40] H. M. Zhang, D. Zhang, X. W. Lu, C. Liu, G. Y. Zhou, X. C. Ma, L. L. Wang, P. Jiang, Q. K. Xue, X. H. Bao, "Origin of charge transfer and enhanced electron–phonon coupling in single unit-cell FeSe films on $SrTiO_3$", *Nat. Commun.* **8** (2017), no. 1, article no. 214.

[41] W. Zhao, M. Li, C.-Z. Chang, J. Jiang, L. Wu, C. Liu, J. S. Moodera, Y. Zhu, M. H. Chan, "Direct imaging of electron transfer and its influence on superconducting pairing at FeSe/$SrTiO_3$ interface", *Sci. Adv.* **4** (2018), no. 3, article no. eaao2682.

[42] P. K. Biswas, Z. Salman, Q. Song, R. Peng, J. Zhang, L. Shu, D. L. Feng, T. Prokscha, E. Morenzoni, "Direct evidence of superconductivity and determination of the superfluid density in buried ultrathin FeSe grown on $SrTiO_3$", *Phys. Rev. B* **97** (2018), article no. 174509.

[43] H. Sims, D. N. Leonard, A. Y. Birenbaum, Z. Ge, T. Berlijn, L. Li, V. R. Cooper, M. F. Chisholm, S. T. Pantelides, "Intrinsic interfacial van der Waals monolayers and their effect on the high-temperature superconductor FeSe/$SrTiO_3$", *Phys. Rev. B* **100** (2019), article no. 144103.

[44] G. Y. Zhou, Q. H. Zhang, F. W. Zheng, D. Zhang, C. Liu, X. X. Wang, C. L. Song, K. He, X. C. Ma, L. Gu *et al.*, "Interface enhanced superconductivity in monolayer FeSe films on MgO(001): charge transfer with atomic substitution", *Sci. Bull.* **63** (2018), no. 12, p. 747-752.

[45] R. Dingle, H. Störmer, A. Gossard, W. Wiegmann, "Electron mobilities in modulation-doped semiconductor heterojunction superlattices", *Appl. Phys. Lett.* **33** (1978), no. 7, p. 665-667.

[46] M. Nakamura, A. Sawa, H. Sato, H. Akoh, M. Kawasaki, Y. Tokura, "Optical probe of electrostatic-doping in an *n*-type Mott insulator", *Phys. Rev. B* **75** (2007), article no. 155103.

[47] S. Badoux, W. Tabis, F. Laliberté, G. Grissonnanche, B. Vignolle, D. Vignolles, J. Béard, D. A. Bonn, W. N. Hardy, R. Liang, "Change of carrier density at the pseudogap critical point of a cuprate superconductor", *Nature* **531** (2016), no. 7593, p. 210-214.

[48] M. P. M. Dean, G. Dellea, R. S. Springell, F. Yakhou-Harris, K. Kummer, N. B. Brookes, X. Liu, Y. J. Sun, J. Strle, T. Schmitt *et al.*, "Persistence of magnetic excitations in $La_{2-x}Sr_xCuO_4$ from the undoped insulator to the heavily overdoped non-superconducting metal", *Nat. Mater.* **12** (2013), no. 11, p. 1019-1023.

[49] F. Baiutti, G. Logvenov, G. Gregori, G. Cristiani, Y. Wang, W. Sigle, P. A. van Aken, J. Maier, "High-temperature superconductivity in space-charge regions of lanthanum cuprate induced by two-dimensional doping", *Nat. Commun.* **6** (2015), article no. 8586.

[50] N. Reyren, S. Thiel, A. D. Caviglia, L. F. Kourkoutis, G. Hammerl, C. Richter, C. Schneider, T. Kopp, A.-S. Rüetschi, D. Jaccard *et al.*, "Superconducting interfaces between insulating oxides", *Science* **317** (2007), no. 5842, p. 1196-1199.

[51] C. Richter, H. Boschker, W. Dietsche, E. Fillis-Tsirakis, R. Jany, F. Loder, L. Kourkoutis, D. Muller, J. Kirtley, C. Schneider *et al.*, "Interface superconductor with gap behaviour like a high-temperature superconductor", *Nature* **502** (2013), no. 7472, p. 528-531.

[52] H. Lee, N. Campbell, J. Lee, T. J. Asel, T. R. Paudel, H. Zhou, J. W. Lee, B. Noesges, J. Seo, B. Park *et al.*, "Direct observation of a two-dimensional hole gas at oxide interfaces", *Nat. Mater.* **17** (2018), no. 3, p. 231-236.

[53] S. Gariglio, M. Gabay, J. Mannhart, J.-M. Triscone, "Interface superconductivity", *Physica C* **514** (2015), p. 189-198.

[54] N. Nakagawa, H. Y. Hwang, D. A. Muller, "Why some interfaces cannot be sharp", *Nat. Mater.* **5** (2006), no. 3, p. 204-209.

[55] Y. W. Xie, Y. Hikita, C. Bell, H. Y. Hwang, "Control of electronic conduction at an oxide heterointerface using surface polar adsorbates", *Nat. Commun.* **2** (2011), article no. 494.

[56] V. T. Tra, J.-W. Chen, P.-C. Huang, B.-C. Huang, Y. Cao, C.-H. Yeh, H.-J. Liu, E. A. Eliseev, A. N. Morozovska, J.-Y. Lin *et al.*, "Ferroelectric control of the conduction at the $LaAlO_3$/$SrTiO_3$ heterointerface", *Adv. Mater.* **25** (2013), no. 24, p. 3357-3364.

[57] R. Arras, V. G. Ruiz, W. E. Pickett, R. Pentcheva, "Tuning the two-dimensional electron gas at the $LaAlO_3$/$SrTiO_3$(001) interface by metallic contacts", *Phys. Rev. B* **85** (2012), article no. 125404.

[58] T. Kim, S.-I. Kim, S. Joo, S. Kim, J. Jeon, J. Hong, Y.-J. Doh, S.-H. Baek, H. C. Koo, "A possible superconductor-like state at elevated temperatures near metal electrodes in an $LaAlO_3/SrTiO_3$ interface", *Sci. Rep.* **8** (2018), no. 1, article no. 11558.

[59] A. Rastogi, S. Tiwari, J. Pulikkotil, Z. Hossain, D. Kumar, R. Budhani, "δ-doped $LaAlO_3$–$SrTiO_3$ interface: Electrical transport and characterization of the interface potential", *EPL* **106** (2014), no. 5, article no. 57002.

[60] A. Ohtomo, D. Muller, J. Grazul, H. Y. Hwang, "Artificial charge-modulationin atomic-scale perovskite titanate superlattices", *Nature* **419** (2002), no. 6905, p. 378-380.

[61] A. Kalabukhov, R. Gunnarsson, T. Claeson, D. Winkler, "Electrical transport properties of polar heterointerface between $KTaO_3$ and $SrTiO_3$", https://arxiv.org/abs/0704.1050, 2007.

[62] Y. Hotta, T. Susaki, H. Y. Hwang, "Polar discontinuity doping of the $LaVO_3/SrTiO_3$ interface", *Phys. Rev. Lett.* **99** (2007), article no. 236805.

[63] T. Koida, M. Lippmaa, T. Fukumura, K. Itaka, Y. Matsumoto, M. Kawasaki, H. Koinuma, "Effect of A-site cation ordering on the magnetoelectric properties in $[(LaMnO_3)_m/(SrMnO_3)_m]_n$ artificial superlattices", *Phys. Rev. B* **66** (2002), article no. 144418.

[64] H. R. Zhang, Y. Yun, X. J. Zhang, H. Zhang, Y. Ma, X. Yan, F. Wang, G. Li, R. Li, T. Khan *et al.*, "High-mobility spin-polarized two-dimensional electron gases at $EuO/KTaO_3$ interfaces", *Phys. Rev. Lett.* **121** (2018), article no. 116803.

[65] C. J. Liu, X. Yan, D. F. Jin, Y. Ma, H. W. Hsiao, Y. Lin, T. M. Bretz-Sullivan, X. J. Zhou, J. Pearson, B. Fisher *et al.*, "Two-dimensional superconductivity and anisotropic transport at $KTaO_3(111)$ interfaces", *Science* **371** (2021), p. 716-721.

[66] P. Cai, W. Ruan, Y. Y. Peng, C. Ye, X. T. Li, Z. Q. Hao, X. J. Zhou, D. H. Lee, Y. Y. Wang, "Visualizing the evolution from the Mott insulator to a charge-ordered insulator in lightly doped cuprates", *Nat. Phys.* **12** (2016), no. 11, p. 1047-1051.

[67] A. Ino, C. Kim, M. Nakamura, T. Yoshida, T. Mizokawa, Z.-X. Shen, A. Fujimori, T. Kakeshita, H. Eisaki, S. Uchida, "Electronic structure of $La_{2-x}Sr_xCuO_4$ in the vicinity of the superconductor-insulator transition", *Phys. Rev. B* **62** (2000), p. 4137-4141.

[68] A. Damascelli, Z. Hussain, Z.-X. Shen, "Angle-resolved photoemission studies of the cuprate superconductors", *Rev. Mod. Phys.* **75** (2003), no. 2, article no. 473.

[69] A. Ino, T. Mizokawa, A. Fujimori, K. Tamasaku, H. Eisaki, S. Uchida, T. Kimura, T. Sasagawa, K. Kishio, "Chemical potential shift in overdoped and underdoped $La_{2-x}Sr_xCuO_4$", *Phys. Rev. Lett.* **79** (1997), p. 2101-2104.

[70] W. Kyung, S. Huh, Y. Koh, K. Y. Choi, M. Nakajima, H. Eisaki, J. D. Denlinger, S. K. Mo, C. Kim, Y. K. Kim, "Enhanced superconductivity in surface-electron-doped iron pnictide $Ba(Fe_{1.94}Co_{0.06})_2As_2$", *Nat. Mater.* **15** (2016), no. 12, p. 1233-1236.

[71] J. Seo, B. Kim, B. S. Kim, J. Jeong, J. Ok, J. S. Kim, J. Denlinger, S. K. Mo, C. Kim, Y. K. Kim, "Superconductivity below 20 K in heavily electron-doped surface layer of FeSe bulk crystal", *Nat. Commun.* **7** (2016), article no. 11116.

[72] X. Shi, Z. Q. Han, X. L. Peng, P. Richard, T. Qian, X. X. Wu, M. W. Qiu, S. C. Wang, J. P. Hu, Y. J. Sun *et al.*, "Enhanced superconductivity accompanying a Lifshitz transition in electron-doped FeSe monolayer", *Nat. Commun.* **8** (2017), article no. 14988.

[73] T. Shimojima, Y. Suzuki, T. Sonobe, A. Nakamura, M. Sakano, J. Omachi, K. Yoshioka, M. Kuwata-Gonokami, K. Ono, H. Kumigashira *et al.*, "Lifting of *xz*/*yz* orbital degeneracy at the structural transition in detwinned FeSe", *Phys. Rev. B* **90** (2014), article no. 121111.

[74] R. Peng, H. C. Xu, S. Y. Tan, H. Y. Cao, M. Xia, X. P. Shen, Z. C. Huang, C. P. Wen, Q. Song, T. Zhang *et al.*, "Tuning the band structure and superconductivity in single-layer FeSe by interface engineering", *Nat. Commun.* **5** (2014), article no. 5044.

[75] D. X. Mou, S. Y. Liu, X. W. Jia, J. F. He, Y. Y. Peng, L. Zhao, L. Yu, G. D. Liu, S. L. He, X. L. Dong *et al.*, "Distinct Fermi surface topology and nodeless superconducting gap in a $Tl_{0.58}Rb_{0.42}Fe_{1.72}Se_2$ superconductor", *Phys. Rev. Lett.* **106** (2011), article no. 107001.

[76] Y. Zhang, L. X. Yang, M. Xu, Z. R. Ye, F. Chen, C. He, H. C. Xu, J. Jiang, B. P. Xie, J. J. Ying *et al.*, "Nodeless superconducting gap in $A_xFe_2Se_2$ (A = K, Cs) revealed by angle-resolved photoemission spectroscopy", *Nat. Mater.* **10** (2011), no. 4, p. 273-277.

[77] L. Fanfarillo, J. Mansart, P. Toulemonde, H. Cercellier, P. Le Fèvre, F. M. C. Bertran, B. Valenzuela, L. Benfatto, V. Brouet, "Orbital-dependent Fermi surface shrinking as a fingerprint of nematicity in FeSe", *Phys. Rev. B* **94** (2016), article no. 155138.

[78] X. P. Wang, T. Qian, P. Richard, P. Zhang, J. Dong, H. D. Wang, C. H. Dong, M. H. Fang, H. Ding, "Strong nodeless pairing on separate electron Fermi surface sheets in $(Tl,K)Fe_{1.78}Se_2$ probed by ARPES", *EPL* **93** (2011), no. 5, article no. 57001.

[79] L. Zhao, D. X. Mou, S. Y. Liu, X. W. Jia, J. F. He, Y. Y. Peng, L. Yu, X. Liu, G. D. Liu, S. L. He *et al.*, "Common Fermi-surface topology and nodeless superconducting gap of $K_{0.68}Fe_{1.79}Se_2$ and $(Tl_{0.45}K_{0.34})Fe_{1.84}Se_2$ superconductors revealed via angle-resolved photoemission", *Phys. Rev. B* **83** (2011), article no. 140508.

[80] T. Qian, X. P. Wang, W. C. Jin, P. Zhang, P. Richard, G. Xu, X. Dai, Z. Fang, J. G. Guo, X. L. Chen *et al.*, "Absence of a holelike Fermi surface for the iron-based $K_{0.8}Fe_{1.7}Se_2$ duperconductor tevealed by angle-resolved photoemission spectroscopy", *Phys. Rev. Lett.* **106** (2011), article no. 187001.

[81] T. Sato, K. Nakayama, Y. Sekiba, P. Richard, Y. M. Xu, S. Souma, T. Takahashi, G. F. Chen, J. L. Luo, N. L. Wang *et al.*, "Band structure and Fermi surface of an extremely overdoped iron-based superconductor KFe_2As_2", *Phys. Rev. Lett.* **103** (2009), article no. 047002.

[82] S. Moser, L. Moreschini, H. Y. Yang, D. Innocenti, F. Fuchs, N. H. Hansen, Y. J. Chang, K. S. Kim, A. L. Walter, A. Bostwick *et al.*, "Angle-resolved photoemission spectroscopy of tetragonal CuO: evidence for intralayer coupling between cupratelike sublattices", *Phys. Rev. Lett.* **113** (2014), article no. 187001.

[83] T. Takeuchi, T. Yokoya, S. Shin, K. Jinno, M. Matsuura, T. Kondo, H. Ikuta, U. Mizutani, "Topology of the Fermi surface and band structure near the Fermi level in the Pb-doped $Bi_2Sr_2CuO_{6+\delta}$ superconductor", *J. Electron. Spectros. Relat. Phenomena* **114** (2001), p. 629-634.

[84] K. M. Shen, F. Ronning, D. H. Lu, W. S. Lee, N. J. C. Ingle, W. Meevasana, F. Baumberger, A. Damascelli, N. P. Armitage, L. L. Miller *et al.*, "Missing quasiparticles and the chemical potential puzzle in the doping evolution of the cuprate superconductors", *Phys. Rev. Lett.* **93** (2004), article no. 267002.

[85] H. Yagi, T. Yoshida, A. Fujimori, Y. Kohsaka, M. Misawa, T. Sasagawa, H. Takagi, M. Azuma, M. Takano, "Chemical potential shift in lightly doped to optimally doped $Ca_{2-x}Na_xCuO_2Cl_2$", *Phys. Rev. B* **73** (2006), article no. 172503.

[86] N. Harima, A. Fujimori, T. Sugaya, I. Terasaki, "Chemical potential shift in lightly doped to overdoped $Bi_2Sr_2Ca_{1-x}R_xCu_2O_{8+y}$ (R = Pr, Er)", *Phys. Rev. B* **67** (2003), article no. 172501.

[87] S. Sahrakorpi, R. S. Markiewicz, H. Lin, M. Lindroos, X. J. Zhou, T. Yoshida, W. L. Yang, T. Kakeshita, H. Eisaki, S. Uchida *et al.*, "Appearance of universal metallic dispersion in a doped Mott insulator", *Phys. Rev. B* **78** (2008), article no. 104513.

[88] A. Ino, C. Kim, M. Nakamura, T. Yoshida, T. Mizokawa, A. Fujimori, Z.-X. Shen, T. Kakeshita, H. Eisaki, S. Uchida, "Doping-dependent evolution of the electronic structure of $La_{2-x}Sr_xCuO_4$ in the superconducting and metallic phases", *Phys. Rev. B* **65** (2002), article no. 094504.

[89] S. Sachdev, M. A. Metlitski, M. Punk, "Antiferromagnetism in metals: from the cuprate superconductors to the heavy Fermion materials", *J. Phys.: Condens. Matter* **24** (2012), no. 29, article no. 294205.

[90] N. Harima, J. Matsuno, A. Fujimori, Y. Onose, Y. Taguchi, Y. Tokura, "Chemical potential shift in $Nd_{2-x}Ce_xCuO_4$: Contrasting behavior between the electron- and hole-doped cuprates", *Phys. Rev. B* **64** (2001), article no. 220507.

[91] N. P. Armitage, F. Ronning, D. H. Lu, C. Kim, A. Damascelli, K. M. Shen, D. L. Feng, H. Eisaki, Z.-X. Shen, P. K. Mang *et al.*, "Doping dependence of an n-type cuprate superconductor investigated by angle-resolved photoemission spectroscopy", *Phys. Rev. Lett.* **88** (2002), article no. 257001.

[92] M. Platé, J. D. F. Mottershead, I. S. Elfimov, D. C. Peets, R. Liang, D. A. Bonn, W. N. Hardy, S. Chiuzbaian, M. Falub, M. Shi *et al.*, "Fermi surface and quasiparticle excitations of overdoped $Tl_2Ba_2CuO_{6+\delta}$", *Phys. Rev. Lett.* **95** (2005), article no. 077001.

[93] A. F. Santander Syro, M. Ikeda, T. Yoshida, A. Fujimori, K. Ishizaka, M. Okawa, S. Shin, R. L. Greene, N. Bontemps, "Two-Fermi-surface superconducting state and a nodal d-wave energy gap of the electron-doped $Sm_{1.85}Ce_{0.15}CuO_{4-\delta}$ cuprate superconductor", *Phys. Rev. Lett.* **106** (2011), article no. 197002.

[94] C. Liu, A. D. Palczewski, R. S. Dhaka, T. Kondo, R. M. Fernandes, E. D. Mun, H. Hodovanets, A. N. Thaler, J. Schmalian, S. L. Bud'ko *et al.*, "Importance of the Fermi-surface topology to the superconducting state of the electron-doped pnictide $Ba(Fe_{1-x}Co_x)_2As_2$", *Phys. Rev. B* **84** (2011), article no. 020509.

[95] L. C. Rhodes, M. D. Watson, A. A. Haghighirad, M. Eschrig, T. K. Kim, "Strongly enhanced temperature dependence of the chemical potential in FeSe", *Phys. Rev. B* **95** (2017), article no. 195111.

[96] R. S. Dhaka, S. E. Hahn, E. Razzoli, R. Jiang, M. Shi, B. N. Harmon, A. Thaler, S. L. Bud'ko, P. C. Canfield, A. Kaminski, "Unusual temperature dependence of band dispersion in $Ba(Fe_{1-x}Ru_x)_2As_2$ and its consequences for antiferromagnetic ordering", *Phys. Rev. Lett.* **110** (2013), article no. 067002.

[97] V. Brouet, P. H. Lin, Y. Texier, J. Bobroff, A. Taleb-Ibrahimi, P. Le Fèvre, F. Bertran, M. Casula, P. Werner, S. Biermann *et al.*, "Large temperature dependence of the number of carriers in Co-doped $BaFe_2As_2$", *Phys. Rev. Lett.* **110** (2013), article no. 167002.

[98] A. Kanigel, M. Norman, M. Randeria, U. Chatterjee, S. Souma, A. Kaminski, H. Fretwell, S. Rosenkranz, M. Shi, T. Sato *et al.*, "Evolution of the pseudogap from Fermi arcs to the nodal liquid", *Nat. Phys.* **2** (2006), no. 7, p. 447-451.

[99] Y. J. Zhou, A. J. Millis, "Charge transfer and electron–phonon coupling in monolayer FeSe on Nb-doped $SrTiO_3$", *Phys. Rev. B* **93** (2016), article no. 224506.

[100] N. Choudhury, E. J. Walter, A. I. Kolesnikov, C. K. Loong, "Large phonon band gap in $SrTiO_3$ and the vibrational signatures of ferroelectricity in $ATiO_3$ perovskites: First-principles lattice dynamics and inelastic neutron scattering", *Phys. Rev. B* **77** (2008), article no. 134111.

[101] F. Li, G. A. Sawatzky, "Electron phonon coupling versus photoelectron energy loss at the origin of replica bands in photoemission of FeSe on $SrTiO_3$", *Phys. Rev. Lett.* **120** (2018), article no. 237001.

[102] Q. Song, T. L. Yu, X. Lou, B. P. Xie, H. C. Xu, C. P. Wen, Q. Yao, S. Y. Zhang, X. T. Zhu, J. D. Guo *et al.*, "Evidence of cooperative effect on the enhanced superconducting transition temperature at the FeSe/$SrTiO_3$ interface", *Nat. Commun.* **10** (2019), no. 1, p. 1-8.

[103] S. Y. Zhang, J. Q. Guan, Y. Wang, T. Berlijn, S. Johnston, X. Jia, B. Liu, Q. Zhu, Q. An, S. Xue *et al.*, "Lattice dynamics of ultrathin FeSe films on $SrTO_3$", *Phys. Rev. B* **97** (2018), article no. 035408.

[104] S. Coh, M. L. Cohen, S. G. Louie, "Large electron–phonon interactions from FeSe phonons in a monolayer", *New J. Phys.* **17** (2015), no. 7, article no. 073027.

[105] Z. Li, J. P. Peng, H. M. Zhang, W. H. Zhang, H. Ding, P. Deng, K. Chang, C. L. Song, S. H. Ji, L. L. Wang *et al.*, "Molecular beam epitaxy growth and post-growth annealing of FeSe films on $SrTiO_3$: A scanning tunneling microscopy study", *J. Phys.: Condens. Matter* **26** (2014), no. 26, article no. 265002.

[106] X. T. Zhu, L. Santos, R. Sankar, S. Chikara, C. Howard, F. C. Chou, C. Chamon, M. El-Batanouny, "Interaction of phonons and Dirac Fermions on the surface of Bi_2Se_3: A strong Kohn anomaly", *Phys. Rev. Lett.* **107** (2011), article no. 186102.

[107] V. Ksenofontov, G. Wortmann, A. I. Chumakov, T. Gasi, S. Medvedev, T. M. McQueen, R. J. Cava, C. Felser, "Density of phonon states in superconducting FeSe as a function of temperature and pressure", *Phys. Rev. B* **81** (2010), article no. 184510.

[108] J. Y. Lin, Y. S. Hsieh, D. A. Chareev, A. N. Vasiliev, Y. Parsons, H. D. Yang, "Coexistence of isotropic and extended *s*-wave order parameters in FeSe as revealed by low-temperature specific heat", *Phys. Rev. B* **84** (2011), article no. 220507.

[109] D. H. Lee, "What makes the T_c of FeSe/$SrTiO_3$ so high?", *Chin. Phys. B* **24** (2015), no. 11, article no. 117405.

[110] K. Liu, B. J. Zhang, Z. Y. Lu, "First-principles study of magnetic frustration in FeSe epitaxial films on $SrTiO_3$", *Phys. Rev. B* **91** (2015), article no. 045107.

[111] Y. T. Cui, R. G. Moore, A. M. Zhang, Y. Tian, J. J. Lee, F. T. Schmitt, W. H. Zhang, W. Li, M. Yi, Z. K. Liu *et al.*, "Interface ferroelectric transition near the gap-opening temperature in a single-unit-cell FeSe film grown on Nb-Doped $SrTiO_3$ substrate", *Phys. Rev. Lett.* **114** (2015), article no. 037002.

[112] S. Y. Zhang, J. Q. Guan, X. Jia, B. Liu, W. H. Wang, F. S. Li, L. L. Wang, X. C. Ma, Q. K. Xue, J. D. Zhang *et al.*, "Role of $SrTiO_3$ phonon penetrating into thin FeSe films in the enhancement of superconductivity", *Phys. Rev. B* **94** (2016), article no. 081116.

[113] S. Y. Zhang, T. Wei, J. Q. Guan, Q. Zhu, W. Qin, W. H. Wang, J. D. Zhang, E. W. Plummer, X. T. Zhu, Z. Y. Zhang *et al.*, "Enhanced superconducting state in FeSe/$SrTiO_3$ by a dynamic interfacial polaron mechanism", *Phys. Rev. Lett.* **122** (2019), article no. 066802.

[114] S. Gerber, S. L. Yang, D. Zhu, H. Soifer, J. Sobota, S. Rebec, J. Lee, T. Jia, B. Moritz, C. Jia *et al.*, "Femtosecond electron–phonon lock-in by photoemission and X-ray free-electron laser", *Science* **357** (2017), no. 6346, p. 71-75.

[115] P. Zhang, X. L. Peng, T. Qian, P. Richard, X. Shi, J. Z. Ma, B. B. Fu, Y. L. Guo, Z. Q. Han, S. C. Wang *et al.*, "Observation of high-T_c superconductivity in rectangular FeSe/$SrTiO_3$(110) monolayers", *Phys. Rev. B* **94** (2016), article no. 104510.

[116] G. Y. Zhou, D. Zhang, C. Liu, C. J. Tang, X. X. Wang, Z. Li, C. L. Song, S. H. Ji, K. He, L. L. Wang *et al.*, "Interface induced high temperature superconductivity in single unit-cell FeSe on $SrTiO_3$(110)", *Appl. Phys. Lett.* **108** (2016), no. 20, article no. 202603.

[117] H. Ding, Y. F. Lv, K. Zhao, W. L. Wang, L. L. Wang, C. L. Song, X. Chen, X. C. Ma, Q. K. Xue, "High-temperature superconductivity in single-unit-cell FeSe films on anatase TiO_2(001)", *Phys. Rev. Lett.* **117** (2016), article no. 067001.

[118] S. N. Rebec, T. Jia, C. Zhang, M. Hashimoto, D. H. Lu, R. G. Moore, Z. X. Shen, "Coexistence of replica bands and superconductivity in FeSe monolayer films", *Phys. Rev. Lett.* **118** (2017), article no. 067002.

[119] H. H. Yang, G. Y. Zhou, Y. Y. Zhu, G. M. Gong, Q. H. Zhang, M. H. Liao, Z. Li, C. Ding, F. Q. Meng, M. Rafique *et al.*, "Superconductivity above 28 K in single unit cell FeSe films interfaced with $GaO_{2-\delta}$ layer on $NdGaO_3$(110)", *Sci. Bull.* **64** (2019), p. 490-494.

[120] Q. S. Wang, Y. Shen, B. Y. Pan, Y. Q. Hao, M. W. Ma, F. Zhou, P. Steffens, K. Schmalzl, T. Forrest, M. Abdel-Hafiez *et al.*, "Strong interplay between stripe spin fluctuations, nematicity and superconductivity in FeSe", *Nat. Mater.* **15** (2016), no. 2, p. 159-163.

[121] L. Kai, G. Miao, L. Zhong Yi, X. Tao, "First-principles study of FeSe epitaxial films on $SrTiO_3$", *Chin. Phys. B* **24** (2015), no. 11, article no. 117402.

[122] H. Y. Cao, S. Chen, H. Xiang, X. G. Gong, "Antiferromagnetic ground state with pair-checkerboard order in FeSe", *Phys. Rev. B* **91** (2015), article no. 020504.

[123] Y. Zhou, L. Miao, P. Wang, F. F. Zhu, W. X. Jiang, S. W. Jiang, Y. Zhang, B. Lei, X. H. Chen, H. F. Ding *et al.*, "Antiferromagnetic order in epitaxial FeSe films on $SrTiO_3$", *Phys. Rev. Lett.* **120** (2018), article no. 097001.

[124] Y. Zhou, A. J. Millis, "Dipolar phonons and electronic screening in monolayer FeSe on $SrTiO_3$", *Phys. Rev. B* **96** (2017), article no. 054516.

[125] L. Li, C. Richter, J. Mannhart, R. Ashoori, "Coexistence of magnetic order and two-dimensional superconductivity at $LaAlO_3$/$SrTiO_3$ interfaces", *Nat. Phys.* **7** (2011), no. 10, p. 762-766.

[126] A. Scholl, J. Stöhr, J. Lüning, J. W. Seo, J. Fompeyrine, H. Siegwart, J.-P. Locquet, F. Nolting, S. Anders, E. Fullerton *et al.*, "Observation of antiferromagnetic domains in epitaxial thin films", *Science* **287** (2000), no. 5455, p. 1014-1016.

[127] T. Bazhirov, M. L. Cohen, "Spin-resolved electron–phonon coupling in FeSe and KFe_2Se_2", *Phys. Rev. B* **86** (2012), article no. 134517.

[128] F. W. Zheng, Z. G. Wang, W. Kang, P. Zhang, “Antiferromagnetic FeSe monolayer on $SrTiO_3$: the charge doping and electric field effects”, *Sci. Rep.* **3** (2013), article no. 2213.
[129] T. Bazhirov, M. L. Cohen, “Effects of charge doping and constrained magnetization on the electronic structure of an FeSe monolayer”, *J. Phys.: Condens. Matter* **25** (2013), no. 10, article no. 105506.
[130] W. T. Zhang, T. Miller, C. L. Smallwood, Y. Yoshida, H. Eisaki, R. Kaindl, D. H. Lee, A. Lanzara, “Stimulated emission of Cooper pairs in a high-temperature cuprate superconductor”, *Sci. Rep.* **6** (2016), article no. 29100.
[131] J. R. Schrieffer, J. S. Brooks, *Handbook of High-temperature Superconductivity: Theory and Experiment*, Springer, New York, NY, USA, 2007.
[132] M. Hepting, L. Chaix, E. Huang, R. Fumagalli, Y. Peng, B. Moritz, K. Kummer, N. Brookes, W. Lee, M. Hashimoto *et al.*, “Three-dimensional collective charge excitations in electron-doped copper oxide superconductors”, *Nature* **563** (2018), no. 7731, p. 374-378.